

Analysis of the discrepancies between high-resolution and low-resolution spectra of the Herschel SPIRE FTS

N. Marchili¹ ...

¹ Dipartimento di Fisica e Astronomia, Università di Padova, I-35131 Padova, Italy
 e-mail: nicola.marchili@gmail.com

²
³

Received ...; accepted ...

ABSTRACT

Key words.

1. Introduction

[...]

The SPIRE FTS allows to take observations in three resolution modes: HR (high resolution; 0.04 cm^{-1}), LR (low resolution; 1.0 cm^{-1}), and H+LR (high resolution scans, followed by low resolution ones). The comparison between the high-resolution and the low-resolution spectra of H+LR observations (from now on, H+LR(H) and H+LR(L), respectively) produced by the standard calibration pipeline of HIPE v11 (reference) reveals the existence of significant discrepancies. Looking at several H+LR observations it appears that, independently of the observed target, this discrepancy — which strongly affects the low-frequency arrays — has a systematic nature; some examples of H+LR(H) and H+LR(L) spectra are shown in Fig. 1, while their differences are shown in Fig. 2. The observed discrepancy always appears like a double bump, with peaks around 550 and 900 GHz.

In the following, the results of a thorough analysis of the problem will be presented; we will focus our attention on the centre detector of the low-frequency array SLWC3. The standard calibration pipeline will be described in Sec. 2, the main results of the comparison of dark sky observations in Sec. 3, a possible analogy with the procedure for the correction of the telescope model in Sec. 4, the analysis of the spectra on a scan-by-scan level in Sec. 5; the open issues and final remarks will be discussed in Sec. 6 and 7, respectively.

2. The standard calibration pipeline

The main issue in approaching the analysis of data taken in different resolution modes is — at which stage of the data calibration does it make sense to compare the data? A proper answer requires a brief introduction to the standard calibration pipeline.

Together with the source signal, the telescope and instrument emissions provide the main contributions to the uncalibrated spectra. These can be expressed in terms of voltage density as

$$V_{\text{Tel}}(\nu) = M_{\text{Tel}}(\nu)R_{\text{Tel}}(\nu) \quad (1)$$

Send offprint requests to: N. Marchili

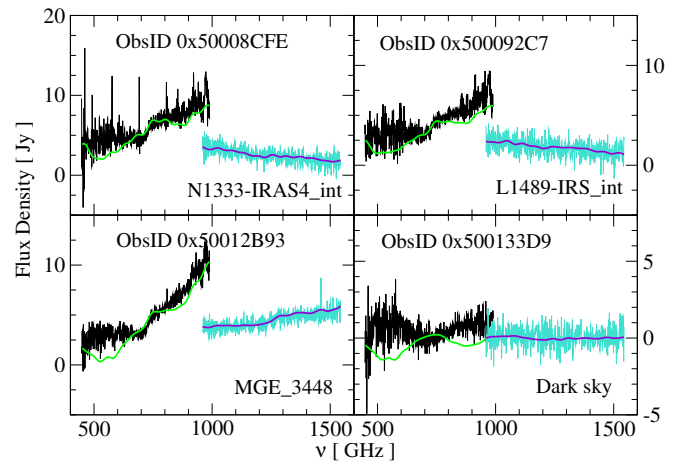


Fig. 1. Some examples of H+LR observations. In green and violet, the low-resolution spectra from detectors SLWC3 and SSWD4, respectively; in black and turquoise, the high-resolution ones.

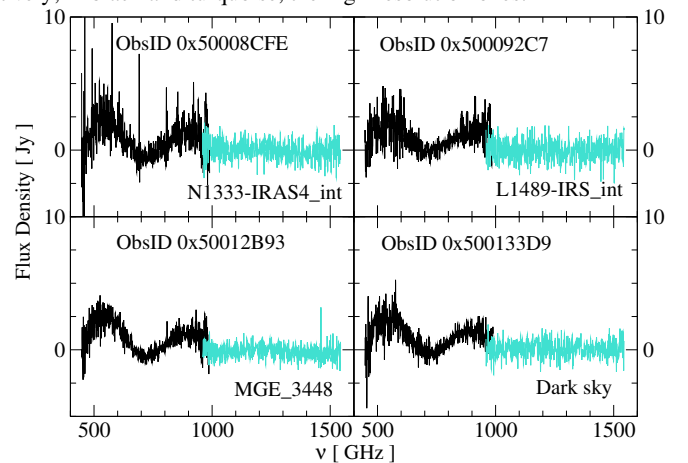


Fig. 2. The difference between the high-resolution and the low-resolution spectra shown in Fig. 1.

and

$$V_{\text{Inst}}(\nu) = M_{\text{Inst}}(\nu)R_{\text{Inst}}(\nu) \quad (2)$$

where $M_{\text{Tel}}(\nu)$ and $M_{\text{Inst}}(\nu)$ are the telescope and instrument models (see ... reference), and $R_{\text{Tel}}(\nu)$ and $R_{\text{Inst}}(\nu)$ the telescope and instrument relative spectral response functions (RSRFs), respectively.

Note that the RSRFs for HR and LR spectra in the standard pipeline are different — their estimation is performed through a procedure that aims at minimizing the residual noise in dark sky observations, for which the telescope and the instrument should provide the only contributions to the spectra. Before HIPE 9, LR calibration was calculated using the low resolution portion of calibration resolution (CR) and HR dark sky observations. This method, however, was not optimal for LR observations, because of the large systematic residuals in the calibrated spectra. For the later versions of HIPE, the calibration of LR spectra has been carried out using a new set of response functions, based on LR dark sky observations. The HR RSRFs, instead, have been calculated by considering HR dark sky observations. Consequently, even assuming that two observations in different resolution modes are taken in the same conditions, i.e. with equal telescope and instrument temperatures, the corrections applied to the respective spectra are different. This leads to a remarkable complication: the uncalibrated HR and LR spectra may not be identical because, even when taken within a very short time interval, the instrument emission may be significantly different for the two. The calibrated spectra, on the other hand, depend on $M_{\text{Tel}}(\nu)$, $M_{\text{Inst}}(\nu)$, $R_{\text{Tel}}(\nu)$, and $R_{\text{Inst}}(\nu)$, which change from version to version of HIPE; moreover, comparing the final spectra does not help to understand the origin of the detected discrepancy.

This issue has been overcome by comparing the high-resolution and low-resolution spectra at every step of the data calibration procedure. It is observed that the difference between the H+LR(H) and H+LR(L) uncalibrated spectra is marginal, implying that the observed discrepancy is introduced in the spectra during the calibration procedure. It also appears that **HR uncalibrated spectra are consistent with both H+LR(H) and H+LR(L) spectra, while the LR ones are systematically different from all the others** (see upper panel of Fig. 3). In the difference between LR and H+LR(L) (black line), it is possible to recognize the double bump already seen in Fig. 2.

It can be inferred that, **while the $R_{\text{Inst}}(\nu)$ function implemented in the pipeline is very efficient in the calibration of LR spectra, it introduces a systematic bias in the calibration of the H+LR(L) spectra**. Significant discrepancies between LR and H+LR data concern not only the uncalibrated spectra, but also interferograms (see lower panel of Fig. 3), and Spectrometer Detector Timelines (SDTs).

3. Comparison of dark sky observations

A fundamental issue must be addressed for investigating the origin of the problem: is the difference between HR/H+LR and LR spectra a constant or does it depend on some parameters, such as, e.g., time, instrument temperature, or telescope temperature? The differences calculated from different pairs of observations (as it will be shown in detail below) are not identical to each other. Partially the observed variations are due to random noise, partially due to other causes that have nothing to do with the resolution modes in which the observations were taken. Beside these two contributions, there might be also variations that *have* to do with the resolution mode, and therefore might be useful to understand the mechanism that causes the discrepancy.

In the following, we will calculate the differences between spectra for specific pairs of observations; these differences

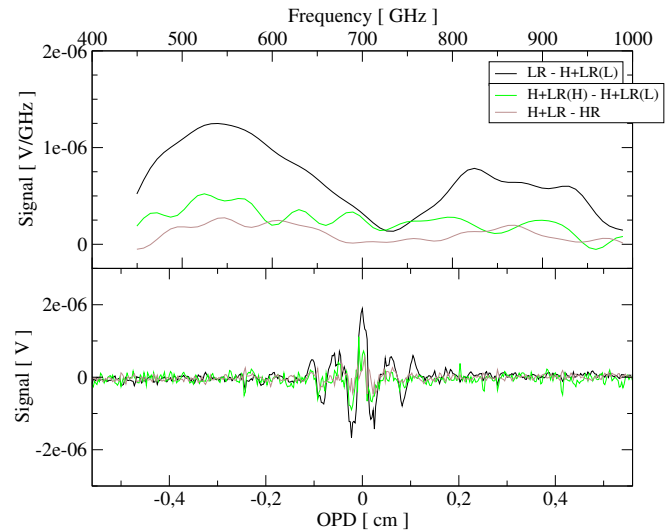


Fig. 3. Upper panel: an example of the differences between the uncalibrated spectra obtained at different resolution modes. Lower panel: the differences seen in the interferograms.

will be referred to as $\delta_{\text{HR-LR}}(\text{ObsID}_{\text{HR/H+LR}}, \text{ObsID}_{\text{LR}})$, where ObsID stands for the identification numbers of the observations. The systematic difference between HR/H+LR and LR spectra, intended as an ideal difference between spectra observed simultaneously and freed from noise and resolution-independent sources of radiation, will be referred to as $\delta_{\text{HR-LR}}$.

The difference $\delta_{\text{HR-LR}}$ has been calculated for a set of quasi-simultaneous dark sky observations performed at different resolution modes. Given the low number of H+LR observations and the similarity between H+LR and HR data, we focused on the comparison between HR and LR dark sky observations. Note that HR observations can be calibrated as if they were taken in low-resolution mode, by cutting HR interferograms at the same optical path difference as LR ones. Most of the LR dark sky observations acquired by the SPIRE FTS are concentrated within the time span between the Observational Days (OD) 1079 and 1433. Before OD 1079, dark sky observations were generally taken in calibration resolution (CR) mode, which is analogous to the HR mode. For the present analysis, we focused on a sample of dark sky observations between OD 1079 and OD 1325. The identification numbers of these observations are listed in Table 1.

From the comparison of the uncalibrated spectra (see Fig. 4), it is easy to recognize the double bump that has been identified as the signature of the discrepancy between HR and LR data. Unfortunately, it is also evident that there is a large spread in the plotted lines, caused by the significant differences in the instrument emissions measured between the LR and the quasi-simultaneous HR observation¹. Again, there seems to be no satisfying way to address the problem: in order to isolate the systematic part of the discrepancy from possible contamination introduced by the instrument and telescope corrections, it would seem reasonable to look at uncalibrated spectra. On the other hand, the differences in the instrument emission between consecutive observations are such that, without instrument correc-

¹ Why this large discrepancy, while almost no difference is seen between H+LR(H) and H+LR(L), as stated in the previous section? It is the order in which the observations are taken that matters. LR observations are almost always taken before HR ones, while, in H+LR observations, the low-resolution scans always follow the high-resolution ones. This point will be further considered later on.

Table 1. Set of dark sky observations used for the present analysis. In Col. 1 we reported the observational day; in Col. 2 and 3 the identification number of the LR and the quasi-simultaneous HR observation, respectively.

OD	ObsID _{LR}	ObsID _{HR}
1079	0x50010904	0x50010905
1098	0x50010BDC	0x50010BDD
1111	0x50010D74	0x50010D75
1125	0x50011047	0x50011048
1130	0x500110C4	0x500110C5
1144	0x50011296	0x50011297
1150	0x50011348	0x50011349
1160	0x5001152A	0x5001152B
1177	0x5001186B	0x5001186C
1186	0x500119ED	0x500119EE
1207	0x50011E15	0x50011E16
1262	0x50012B95	0x50012B94
1283	0x500130A4	0x500130A5
1291	0x500133D5	0x500133DB
1291	0x500133D6	0x500133DB
1291	0x500133D8	0x500133DB
1298	0x500134E8	0x500134E9
1313	0x500138B6	0x500138B7
1325	0x50013B00	0x50013B01

tion, $\delta_{\text{HR-LR}}$ can still not be properly evaluated. The similarity between the spectra obtained after the instrument correction (see Fig. 5) suggests that the latter approach leads to a better estimate of $\delta_{\text{HR-LR}}$.

The modest fluctuations among the $\delta_{\text{HR-LR}}$ curves obtained at different ODs seem to indicate that, at least in first approximation, the discrepancy between LR and HR/H+LR spectra can be regarded as constant in time. This hypothesis has been tested by developing a calibration procedure which adds to the two standard contributions, from the telescope and the instrument, a third one which does not depend on time (and therefore neither on temperature); the three parameters of this new model are calculated simultaneously.

3.1. Three-parameter model for the calibration of the data

The measured voltage density V_i for a dark sky observation i has been expressed as

$$V_i(\nu) = M_{\text{Tel}}(\nu)R_{\text{Tel}}'(\nu) + M_{\text{Inst}}(\nu)R_{\text{Inst}}'(\nu) + f(\nu). \quad (3)$$

For each of the observations in Table 1, the variables $V_i(\nu)$, $M_{\text{Tel}}(\nu)$, and $M_{\text{Inst}}(\nu)$ are known. Given the 19 LR (17 HR) observations at our disposal, for each frequency a system of 19 (17) equations with three unknowns can be build to calculate the best-fit parameters for LR (HR) data. Since the systems are overdetermined, a least-square fitting algorithm is used to simultaneously estimate $R_{\text{Tel}}'(\nu)$, $R_{\text{Inst}}'(\nu)$, and $f(\nu)$. The results are plotted in Fig. 6

The differences between the best fit parameters for LR and HR data are not limited to $f(\nu)$. Similarly to the standard pipeline, we find that when using a three-parameter model **the RSRFs at different resolution modes are not consistent among each other**. In Fig. 7, the differences between the contributions at different resolution modes provided by each of the three components on the right-hand side of Eq. 3 are shown. Remarkably, the difference on $f(\nu)$ shows the same double bump as seen in $\delta_{\text{HR-LR}}$, with an amplitude that is one order of mag-

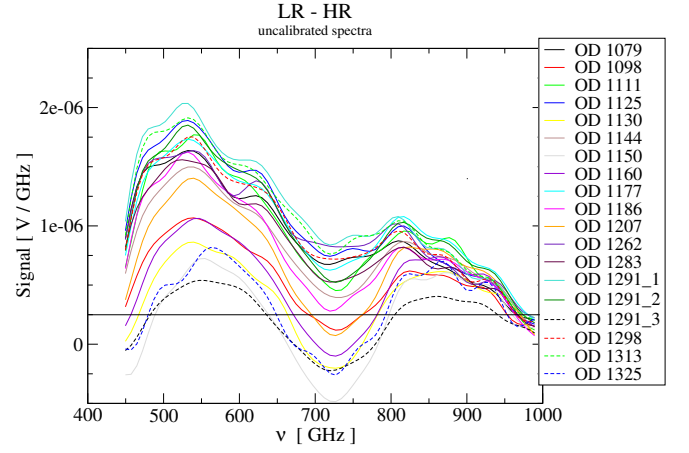


Fig. 4. Difference between quasi-simultaneous LR and HR spectra. The relatively large spread between the lines is caused by the uncorrected instrument emission.

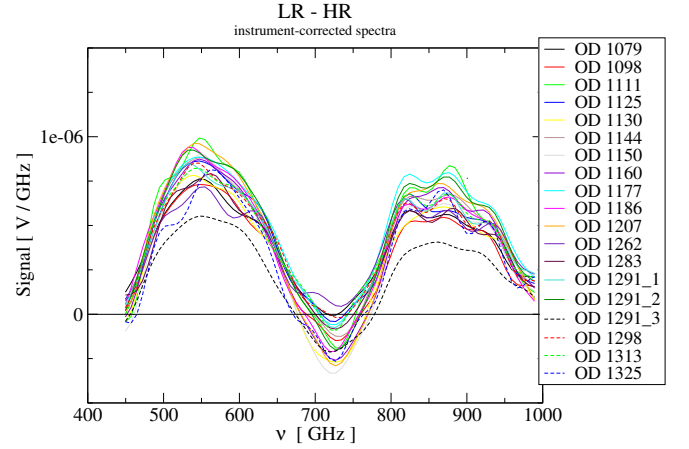


Fig. 5. Difference between quasi-simultaneous LR and HR spectra, after applying the instrument correction.

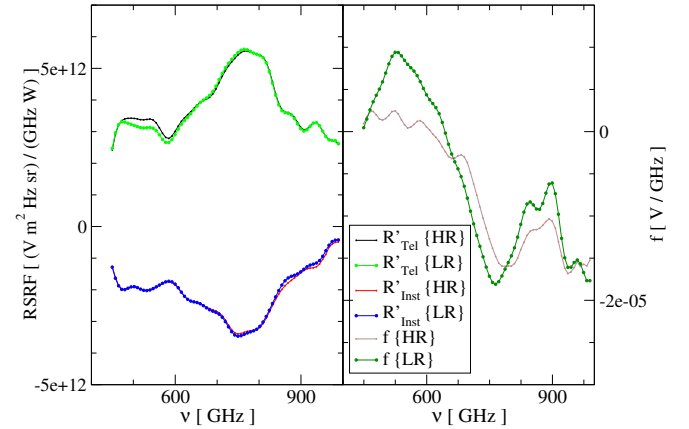


Fig. 6. The best fit RSRFs (left panel) and the $f(\nu)$ parameter (right panel) estimated from the 19 LR and 17 HR dark sky observations in Table 1. The HR spectra utilized for calculating the parameters have been produced in low-resolution mode using the specific option in the data reduction pipeline.

nitude higher; large part of this contribution is cancelled out by the opposite behavior of the telescope correction.

This result has two important consequences: i) we regarded $\delta_{\text{HR-LR}}$ as a constant, but this assumption is correct only in first approximation; the discrepancies in the response functions at

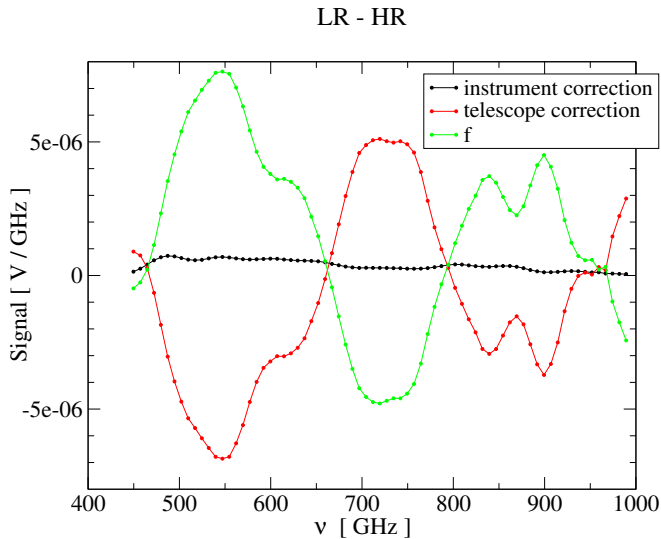


Fig. 7. Average differences between the correction curves for LR and HR data.

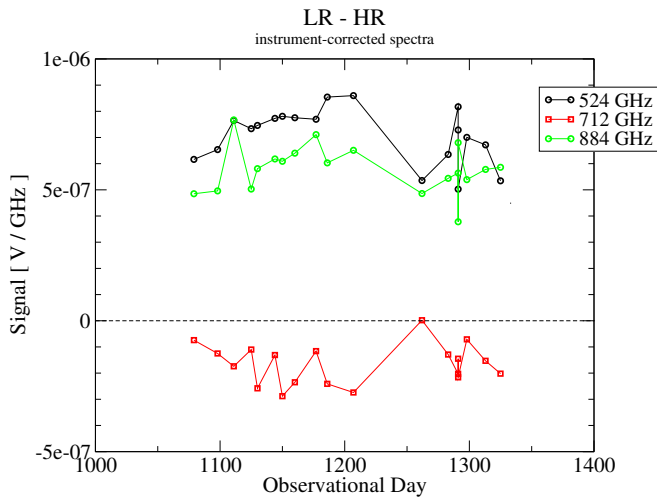


Fig. 8. The temporal evolution of $\delta_{\text{HR-LR}}(\text{ObsID}_{\text{HR}}, \text{ObsID}_{\text{LR}})$ at three different frequencies: 524 GHz (black dots), 712 GHz (red squares), and 884 GHz (green dots).

different resolutions imply that the amplitude of the discrepancy must depend on the instrument and telescope temperatures. ii) The existence of $\delta_{\text{HR-LR}}$ cannot be attributed to systematically wrong estimates of the telescope or instrument temperatures, because no systematic temperature variation could mimic a difference in the RSRFs.

Both conclusions are evident from Fig. 8, where the differences $\delta_{\text{HR-LR}}(\text{ObsID}_{\text{HR}}, \text{ObsID}_{\text{LR}})$ at frequencies of 524 and 884 GHz (black and green dots) — close to the local maxima of the discrepancy —, are compared with the ones at 712 GHz (red squares) — around the minimum of the discrepancy — for the sets of observations in Table 1. While the variations at 524 and 884 GHz show correlated trends, the pattern followed by the variations at 712 GHz is approximately antithetical. Therefore the variations of $\delta_{\text{HR-LR}}(\text{ObsID}_{\text{HR}}, \text{ObsID}_{\text{LR}})$ are proportional to $\delta_{\text{HR-LR}}$, which means that the variability is intrinsic to $\delta_{\text{HR-LR}}$. Also, it would not be possible to simultaneously correct for the variations at 524, 712, and 884 GHz by modifying the telescope or the instrument model, as it would cause coherent signal variations at all frequencies.

Table 2. Dark sky observations carried out in OD 1291 (Col. 1), with their resolution modes (Col. 2) and number of repetitions (Col. 3).

Obsid	Resolution mode	Reps
0x500133D5	LR	20
0x500133D6	LR	20
0x500133D7	HR	5
0x500133D8	LR	20
0x500133D9	H+LR	25
0x500133DB	HR	70

3.2. Dark sky observations in OD 1291

A difference between the response functions at low and high resolution implies that the same radiation from the instrument or the telescope produces different contributions to the LR and HR spectra. This would point toward a different sensitivity of the mechanics or the optics to the resolution mode, which seems quite unlikely. Some interesting indications are provided by a set of dark sky observations carried out in OD 1291, performed in LR, HR, and H+LR resolution modes (see Table 2).

Given the short time interval between the observations, the telescope contribution to the flux is expected to be approximately constant. The difference between instrument corrected spectra of all the observations from 0x500133D5 to 0x500133D9 and the one of obsid 0x500133DB are plotted in the lower panel of Fig. 9.

Several points deserve to be noted:

- depending on the temporal sequence in which they are observed, distinct HR and LR spectra are sometimes perfectly compatible among each other (see the spectra for obsids 0x500133D7 and 0x500133D8); this is consistent with the negligible differences seen between H+LR(H) and H+LR(L);
- the differences among high-resolution spectra can be similar in shape and comparable in amplitude to $\delta_{\text{HR-LR}}$, as the subtraction of the high-resolution spectra of obsid 0x500133DB from the ones of obsids 0x500133D7 and 0x500133D9 shows;
- low resolution spectra show important variations from one observation to another.

All these arguments point towards excluding that the resolution mode is the direct cause of the problem. The differences with respect to the 0x500133DB spectrum are all characterized by the typical double bump of $\delta_{\text{HR-LR}}$, but the amplitude of the effect varies considerably. Inspecting the housekeeping products for this set of observations, most of the parameters seem to show very mild variations with time (above all, the telescope model). Fast variability can instead be detected in the instrument temperature. Looking at its behaviour during the data acquisition (upper panel of Fig. 9), it is hard to find a unequivocal pattern: i) Most of the spectra seem to gradually tend toward a decreasing difference with respect to the 0x500133DB one, which could suggest a time dependence of the amplitude of the effect; however, the transition from obsid 0x500133D5 to 0x500133D6 seems to go in the opposite direction. ii) Obsid 0x500133D6 is characterized by a positive temperature gradient and a larger departure from obsid 0x500133DB, while the low-resolution spectra 0x500133D8 and 0x500133D9 by negative temperature gradients and proportionally smaller discrepancies from obsid 0x500133DB. A correlation between gradients and amplitude of the effect, however, could apply only to low-resolution data, because the high-resolution observations 0x500133D8 and 0x500133D9 seem to

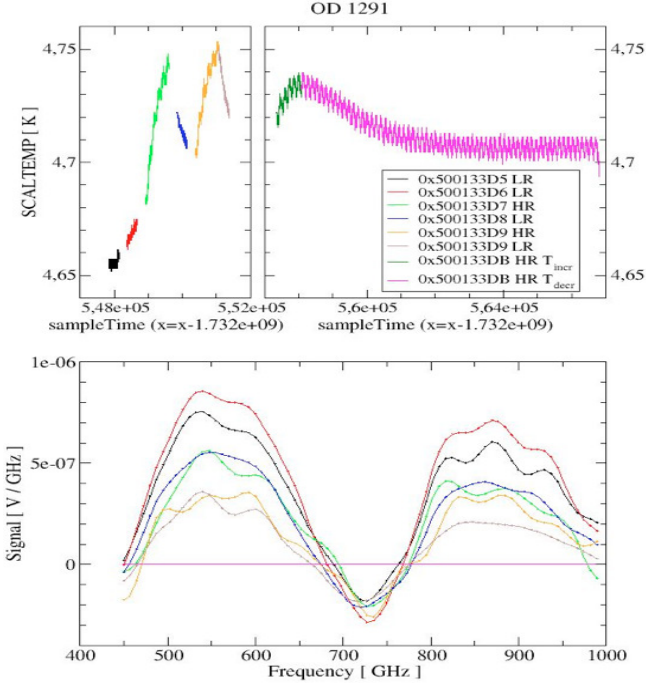


Fig. 9. Upper panel: The variation of the instrument temperature, measured by one of the dedicated sensors, during the observations in OD 1291. Lower panel: the spectra of the observations from 0x500133D5 to 0x500133D9, after subtracting the spectrum of observation 0x500133DB.

contradict it. iii) The most evident distinction between observation 0x500133DB and all the others is the number of repetitions and the duration of the data acquisition. While the 70 repetitions that the former comprises allow the instrument temperature to reach an approximately constant value, observations from 0x500133D6 to 0x500133D9 show strong temperature gradients; this does not apply to obsid 0x500133D5, which is short, but does not show important instrument temperature variations. **In summary, the discrepancies among the spectra are not connected to the instrument temperature in a straightforward way; the number of repetitions of the observations seems to have a significant influence on the measured flux densities.**

4. A link to the telescope model correction?

The hypothesis of a relationship between number of repetitions of an observation and the amplitude of the discrepancy with respect to an average HR spectrum is particularly interesting when confronted with the result of an independent study about the calibration of the SPIRE FTS data, namely the telescope model correction (Hopwood et al. 2013). This study, which takes into account high-resolution spectra, demonstrates the significant improvement of the calibration results after multiplying the telescope model by a time-dependent factor; it is hypothesized that the correction is required because of an extra-emission caused by dust on the surface of the telescope. It is also shown that the correction factor changes according to the number of repetitions of the observation: observations with < 20 repetitions require a higher correction factor than those with > 20 repetitions (see Fig. 5 and 6 in Hopwood et al. 2013). The authors hypothesize that this difference is caused by a higher than average observing temperature (most of the short dark sky observations were

taken at the end of an FTS observing cycle, when the temperatures are generally higher). However, provided that the duration of an observation correlates with the number of repetitions, it might also be that the dependence of the correction factor on the number of repetitions is a dependence on the *duration* of the observation. Since low-resolution observations are systematically shorter than the high-resolution ones, it follows that **the discrepancy between HR and LR data may be one aspect of a more general problem that has to do with the duration of an observation, rather than its resolution mode.**

From the discussion above, one might wonder if the origin of $\delta_{\text{HR-LR}}$ is not the telescope model itself. The multiplication of the original model by a correction factor can translate into a change of the telescope RSRF, which would be compatible with the results reported in Sec. 3.1, but only up to some point. Hypothesizing the existence of two different, slowly-varying correction factors for observations of different duration, the difference between their spectra as a function of frequency should be expressed as $(M_{\text{Tel}}(\nu) - M'_{\text{Tel}}(\nu))R_{\text{Tel}}(\nu)$, where $M_{\text{Tel}}(\nu)$ and $M'_{\text{Tel}}(\nu)$ would be the different telescope models to apply. Since we know how $M_{\text{Tel}}(\nu)$ varies as a function of ν , we can approximately guess the shape of the difference between the spectra. Such shape is not compatible with the double bump characterizing $\delta_{\text{HR-LR}}$. Inverting the problem, though, **we could still hypothesize that the detected difference between the correction factors is the consequence of observation-duration-dependent RSRFs.**

5. RSRFs calculation from scans of the same observation

The differences among the quasi-simultaneous dark sky observations in OD 1291 demonstrate that possible variations of the RSRFs should occur on short timescales — of the order of minutes. A way to investigate such short-term variations is to analyze the spectra of single scans rather than complete observations. In the following we will focus on the flux densities at a frequency of 524 GHz, around which the discrepancy between LR and HR/H+LR data is most pronounced.

In Fig. 10, the uncalibrated 524 GHz flux density of scans from observations 0x500133D9 and 0x500133DB have been corrected for the telescope emission and plotted versus the instrument model. According to Eq. 3, the data-points should fall along a straight line, whose slope should provide $R_{\text{Inst}}'(524 \text{ GHz})$; note that changes in the telescope model during the observations should be minimal, therefore hardly responsible for any deviation from the expected behavior. For comparison, the plot also reports data-points (black dots) and slope (black line) for the LR observations in Table 1.

The high-resolution part of obsid 0x500133D9 (orange diamonds) is the first in order of time; during these ten scans the instrument temperature increases almost monotonically. The data-points for the first three scans are consistent with the average behavior of low-resolution observations. As the temperature further increases, the decrease in $V_i(\nu) - M_{\text{Tel}}R_{\text{Tel}}'$ becomes much steeper than expected. The average $R_{\text{Inst}}'(524 \text{ GHz})$ (orange line) for the ten scans under consideration indicates that the response of the detector to the instrument emission has changed, leading to a discrepancy with respect to the LR observations.

Afterwards, the low-resolution part of obsid 0x500133D9 (brown dots) is performed, and the instrument temperature tend to decrease. The average $R_{\text{Inst}}'(524 \text{ GHz})$ inferred by a linear regression on these scans (brown line) is very similar — although

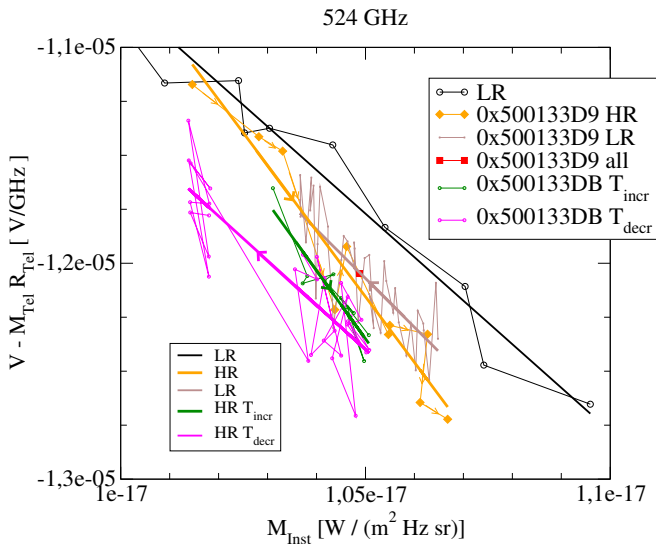


Fig. 10. Telescope-corrected signal at 524 GHz plotted versus the instrument model for samples of scans of ObsIDs 0x500133D9 and 0x500133DB (orange, brown, green, and magenta dots); in black dots, the telescope-corrected signal of all the LR observations in Table 1.

Table 3. The instrument response functions R_{Inst}' inferred from different sets of scans of Obsids 0x500133D9 and 0x500133DB, compared with the one of all LR observations in Table 1; the sets of scans are selected according to the resolution mode and the monotonic trend of the instrument model variation.

Obsid	Resolution mode	M_{Inst}	R_{Inst}'
all LR	LR	—	-2.0163e+12
0x500133D9	HR	increasing	-3.0424e+12
0x500133D9	LR	decreasing	-2.2629e+12
0x500133DB	HR	increasing	-3.1527e+12
0x500133DB	HR	decreasing	-2.0601e+12

slightly steeper — to the one inferred from LR observations, which explains why the discrepancy introduced by the high-resolution part of the observation is approximately preserved. Note the alignment between the flux density for the complete observation (red square) and the fit to these low-resolution datapoints.

The scans of the HR obsid 0x500133DB have been divided in two parts: the ones for which M_{Inst} increases (from now on, 91_{incr}, green dots) and the ones for which it decreases (91_{decr}, magenta dots). When the observation starts, the instrument temperature is higher than at the beginning of obsid 0x500133D9, and the values of $V_i(\nu) - M_{\text{Tel}}R_{\text{Tel}}'$ for the first scans of the two observations are shifted. The slope with which $V_i(\nu) - M_{\text{Tel}}R_{\text{Tel}}'$ decreases with M_{Inst} is again steeper (green line) than the one inferred from LR data and very similar to the one calculated for the high-resolution part of obsid 0x500133D9, so that the difference between the 524 GHz flux density of obsid 0x500133DB and the one expected for LR data increases. Similarly to what we saw for the low-resolution part of obsid 0x500133D9, also the 91_{decr} scans tend to preserve a similar $R_{\text{Inst}}'(524\text{GHz})$ (magenta line) than LR observations.

It might be helpful to summarize the main conclusions from this analysis; in Table 3, for all the sets of scans under consideration (Col. 1), we reported the resolution mode (Col. 2), the behavior of M_{Inst} during the scans (Col. 3), and the inferred R_{Inst}' (Col. 4). It appears that there is a link between R_{Inst}' (which has a direct influence on the measured flux density at 524 GHz) and

the variation of M_{Inst} . The resolution mode, instead, seems not to directly affect the instrument response function.

The picture that comes into view could be the following: slow changes of the instrument temperature cause variations of the voltage density $V_i(\nu)$ which can be generally described as $M_{\text{Inst}}(\nu)R_{\text{Inst,LR}}(\nu)$; the execution of scans in high-resolution mode causes at first a fast increase of the instrument temperature, which produces a change in the instrument response function, leading to an augmented deviation of the measured flux density from the one of standard low-resolution observations. After some high-resolution scans, the instrument temperature stabilizes and eventually decreases again. The instrument response function tends to a value slightly steeper than $R_{\text{Inst,LR}}(\nu)$, approximately preserving the flux density difference introduced by the previous scans. Since the absolute value of the response function for these scans (characterized by rapidly decreasing instrument temperature) is a little higher than $R_{\text{Inst,LR}}(\nu)$, for some value of $M_{\text{Inst}}(\nu)$ ² the instrument emission will equalize $M_{\text{Inst}}(\nu)R_{\text{Inst,LR}}(\nu)$, returning to the starting point of the cycle. As in an hysteresis cycle, the instrument contribution to $V_i(\nu)$ depends on the evolution of the instrument temperature — the way it changed also in previous observations.

5.1. Extending the scan-by-scan analysis to a large sample of HR observations

To probe this hypothesis, the scan-by-scan analysis discussed above has been extended to a sample of 21 HR observations. Since the strongest temperature variations concern the first 20–30 scans of each observation, our analysis is limited to the first 30 and the last 10 scans only. The results are reported in Fig. 11 and 12, where the telescope-corrected signal is plotted versus the instrument model. The green and the orange dotted lines show the typical relationship between signal and instrument model for LR and HR spectra, respectively. Two distinct kinds of behavior can be recognized:

- In eleven cases (see Fig. 11), the signal evolves with the changing temperature according to a clearly recognizable pattern. It starts from a position that is compatible with typical LR spectra; after few scans, it rapidly moves toward a lower state, indicating that the contribution of the instrument emission to the signal is higher than expected for the measured temperature. When the instrument temperature starts to decrease, the signal is generally moving along the orange line that characterizes HR spectra. By overlapping the patterns followed by the eleven observations under consideration, a model of the resulting U-shaped pattern has been obtained (magenta line in the box; its time evolution is clockwise).
- For ten observations (see Fig. 12), the variation of the signal with the changing temperature does not follow a clear trend. The signal seem to approximately start and move along the typical HR line, without significant deviations.

To understand the origin of the differences in behavior between the two samples of observations, it is useful to place them into the framework of their historical sequence. Eight out of eleven observations in the first group have been performed after LR observations, while all the observations in the second group follow HR observations. This result strongly supports the idea that the discrepancies in the calibrated spectra of observations

² Likely, this will happen on much longer timescales than the duration of standard observations.

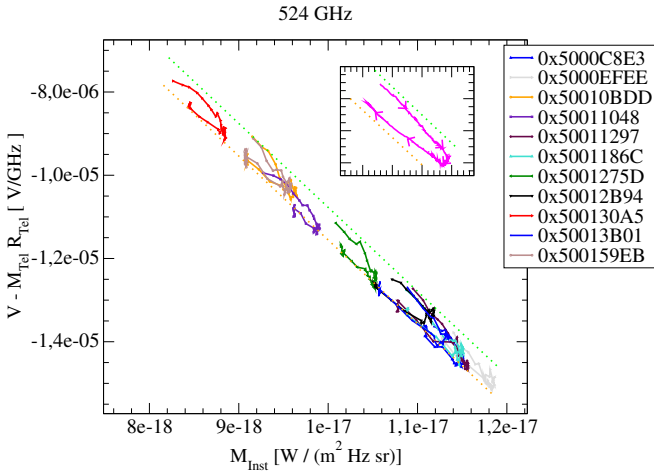


Fig. 11. Telescope-corrected signal at 524 GHz plotted versus the instrument model for samples of scans of HR observations. The signal follows a kind of U-shaped pattern (a model of this pattern is shown as a magenta line in the top-right box), moving clockwise from a typical LR behavior (green dotted line) to a typical HR one (orange dotted line).

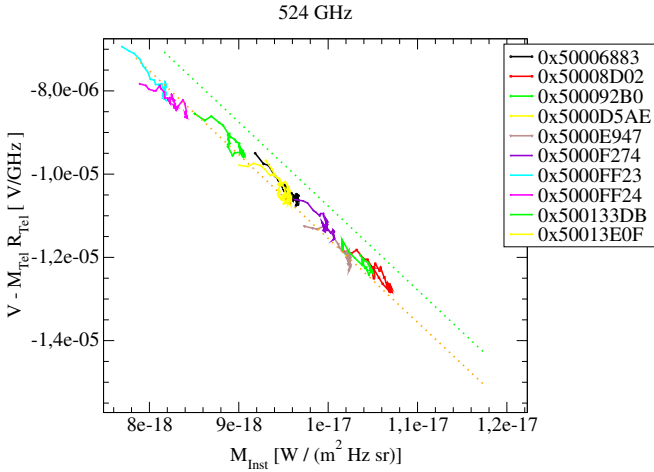


Fig. 12. The evolution of the telescope-corrected signal at 524 GHz for a different group of HR observations. All the scans seem approximately to move along the typical HR line.

performed in different resolution modes has to do with fast variations of the instrument temperature. When temperature variations are slow (as during or after LR scans), the instrument contribution to the signal follows the typical LR line, while sudden increases of the temperature shift it toward the HR line. If two or more HR observations are taken in sequence, the system does not have the time to return to the initial state and all the scans will evolve following the typical HR pattern.

The scenario above provides a coherent description of the variations observed in a large sample of dark sky spectra; it does not explain, though, the origin of the problem. **Comparing the temperatures reported by the three sensors placed in different positions within the instrument (scalTemp, scalTemp2, and scalTemp4) we see a significant delay between the variations triggered by the first scans of each high-resolution observation. It could be an indication that the problem has to do with the thermal balance of the system; the question to address, then, is whether thermal balance can influence the response functions.**

6. Open issues

Through the analysis illustrated in the previous sections it has been possible to highlight several interesting aspects concerning the systematic discrepancy between LR and HR/H+LR data; but rather than providing a uniform picture and allowing to pinpoint the origin of the problem, the collected clues seem to be partially contradictory.

The calculation of the RSRFs separately for HR and LR observations (see Section 3.1) shows that, changing the resolution mode, the telescope contribution to $V_i(\nu)$ varies much more than the instrument contribution (see Fig. 7). Moreover, the dependence of the telescope correction factor on the number of repetitions would naturally suggest a link with the observation-duration dependent variation of the telescope RSRF hypothesized above (see Section 4). These two points would argue in favor of a strong involvement of the telescope emission in the flux density discrepancies. On the other hand, the telescope temperature seems to be nearly constant on timescales from minutes to few hours, excluding its strong involvement in the variations of the spectra acquired in OD 1291; this conclusion is also supported by the possibility to trace these variations as a function of the instrument temperature evolution.

As for now, a final conclusion concerning the origin of $\delta_{\text{HR-LR}}$ is impossible. The most likely scenario seems to be a change of the response functions triggered by the instrument temperature: since HR observations are characterized by temperatures that are generally higher than those of LR observations, the systematic nature of the discrepancy would be explained. Assuming that the instrument temperature affects the telescope RSRF as well as the instrument RSRF, also the analogies found with some characteristics of the telescope correction would be justified. What is still missing is a physical interpretation of changes occurring in the response functions.

7. Final remarks

In the present paper, a thorough analysis of the systematic discrepancy between spectra obtained at different resolution modes has been presented. The discrepancy — detected in the fully calibrated H+LR(H) and H+LR(L) spectra — originates in a systematic difference between uncalibrated LR and HR/H+LR spectra, which the standard calibration pipeline partially corrects by assuming different response functions for LR and HR data.

We tested the hypothesis that the discrepancy, $\delta_{\text{HR-LR}}$, is constant in time, and therefore it can be corrected by adding a constant parameter to the standard two-parameter calibration pipeline. The test showed that, in first approximation, the amplitude of the discrepancy can be regarded as constant, allowing for an empirical correction of the problem by subtracting a constant signal from the uncalibrated spectra of LR observations; however, a minor part of the discrepancy is certainly affected by the (time-dependent) telescope and instrument temperatures. Given the shape of $\delta_{\text{HR-LR}}$ (which shows an excess of signal around 550 and 900 GHz, and a deficiency of signal around 700 GHz), a proper correction of the problem can not be achieved by modifying the telescope and/or the instrument model; it would require a modification of the response functions.

The analysis of the variations in dark sky observations spectra performed in OD 1291, even on a scan-by-scan level, seems to indicate that the amplitude of the discrepancy is not *directly* related to neither the instrument temperature nor its increasing/decreasing trend — it seems to be affected also by the history of the temperature variations before the start of the observation.

The extension of the scan-by-scan analysis to a sample of 21 HR observations strongly supports this conclusion.

We hypothesize that the existence of $\delta_{\text{HR-LR}}$ has to do with fast temperature changes in the instrument, which cause temporary variations of both the telescope and the instrument response functions. The sensitivity of the telescope response function to the instrument temperature may also explain the important analogies observed between some characteristics of $\delta_{\text{HR-LR}}$ and the telescope emission, such as the dependence on the number of repetitions (and consequently the duration) of an observation.

8. Post Scriptum

We have been wondering why spectra obtained at different resolution modes show significant discrepancies. Maybe the most important question would have been how the response functions estimated for LR and HR data in the standard pipeline could be so different among each other. Once we accept that response functions depend on resolution mode, the signals that we expect for given values of the telescope and the instrument models would be resolution dependent:

$$V_{\text{LR}}(\nu) - V_{\text{HR}}(\nu) = M_{\text{Tel}}(\nu)(R_{\text{Tel,LR}}(\nu) - R_{\text{Tel,HR}}(\nu)) + M_{\text{Inst}}(\nu)(R_{\text{Inst,LR}}(\nu) - R_{\text{Inst,HR}}(\nu)) \quad (4)$$

This implies that $V_{\text{LR}}(\nu) - V_{\text{HR}}(\nu)$ cannot be zero unless the telescope and the instrument models show a significant dependence on resolution too. It is not by chance that the problem becomes evident with H+LR observations, for which the instrument and telescope models vary in a negligible way from the high- to the low-resolution part of the observations.

References